JOURNAL OF THEORETICAL AND APPLIED MECHANICS
50, 2, pp. 653-673, Warsaw 2012
50th Anniversary of JTAM

DYNAMIC INVESTIGATIONS OF ELECTROMECHANICAL COUPLING EFFECTS IN THE MECHANISM DRIVEN BY THE STEPPING MOTOR

Tomasz Szolc

Institute of Fundamental Technological Research, Polish Academy of Sciences, and Warsaw University of Technology, Faculty of Mechatronics, Warsaw, Poland
e-mail: tszolc@ippt.gov.pl; t.szolc@mchtr.pw.edu.pl

Andrzej Pochanke

Warsaw University of Technology, Faculty of Electrical Engineering, Warsaw, Poland
e-mail: andrzej.pochanke@ee.pw.edu.pl

In the paper, an analysis of transient and steady-state electro-mechanical vibrations of a precise drive system driven by a stepping motor is performed. These theoretical investigations are based on a hybrid structural model of the mechanical system as well as on the classical circuit model of the stepping motor. The main purpose of these studies is to indicate essential differences between the torsional dynamic responses obtained for the considered object regarded respectively as electro-mechanically coupled and uncoupled. From the computational results, it follows that these differences are qualitatively and quantitatively essential from the viewpoint of possibly precise and reliable operation of the drive systems. Here, torsional vibrations of the drive system significantly influence the electro-mechanical coupling effects, which emphasizes their importance in dynamic analyses.

Key words: electro-mechanical vibrations, drive system, stepping motor, hybrid model

1. Introduction

The drive systems of machines, vehicles as well as of precise mechanisms are commonly driven by electric motors of various types, e.g. asynchronous motors, synchronous motors, several direct-current (DC) motors or stepping motors. During nominal and steady-state operating conditions these motors generate

more or less significant variable components of the electromagnetic torques which are sources of severe torsional vibrations of the entire mechanical drive system. Such torsional vibrations are very dangerous not only from the material fatigue viewpoint, but in some cases they can lead to rapid damages of shafts and couplings in the drive systems. This important problem was studied many years ago by numerous authors, e.g. by Berger and Kulig (1981), Evans *et al.* (1985), Iwatsubo *et al.* (1986), Schwibinger and Nordmann (1989) and many others as well as quite recently, e.g. by Pochanke and Bodnicki (2002), Repo *et al.* (2008), Holopiainen *et al.* (2010), Szolc *et al.* (2010) and others. Torsional vibrations of drive systems usually result in a significant fluctuation of the rotational speed of the rotor of the driving electric motor. Such oscillations of the angular velocity superimposed on the average rotor rotational speed cause more or less severe perturbation of the electro-magnetic flux and thus additional oscillations of the electric currents in the motor windings. Then, the generated electromagnetic torque is also characterised by additional variable in time components which induce torsional vibrations of the drive system. According to the above, mechanical vibrations of the drive system become coupled with the electrical vibrations of currents in the motor windings. Such a coupling is often complicated in character and thus computationally troublesome. Because of this reason, till present majority of authors used to simplify the matter regarding mechanical vibrations of drive systems and electric current vibrations in the motor windings as mutually uncoupled. Then, the mechanical engineers apply the electromagnetic torques generated by the electric motors as *a priori* assumed excitation functions of time or of the rotor-to-stator slip, e.g. in Evans *et al.* (1985), Laschet (1988) and Schwibinger and Nordmann (1989), usually basing on numerous experimental measurements for the given electric motor dynamic behaviour. For this purpose, by means of measurement results, proper approximate formulas are developed which describe respective electromagnetic external excitations produced by the electric motor, Laschet (1988). However, the electricians thoroughly model electric current flows in the electric motor windings, but they usually reduce the mechanical drive system to one or seldom to a few rotating rigid bodies, Sochocki (1996). In many cases, such simplifications yield sufficiently useful results for engineering applications, but very often they can lead to drastic inaccuracies. Therefore, in the literature, one can find some attempts to regard the electric motor-drive system interactions as a coupled dynamic electromechanical problem. For example, in Berger and Kulig (1981), transient torsional vibrations in the turbogenerator sets caused by network disturbances were considered as the rotor-shaft torsional vibrations coupled with the electric current vibrations

in the generator windings. Coupling effects between the geared drive system torsional vibrations and the electric current oscillations in the synchronous motor windings were investigated in Iwatsubo *et al.* (1986), where the current flows in the electric machine windings were modelled using Park's equations. Coupled electromechanical interactions were studied in Pochanke and Bodnicki (2002) for the stepping motor driving a torsional train modelled by means of two rigid bodies mutually connected by a mass-less torsional spring. In Repo *et al.* (2008) and Holopainen *et al.* (2010), the dynamic interaction between the asynchronous and synchronous motors and the drive system was studied, where the motor electro-magnetic flux was modelled using three dimensional finite elements and the drive train was substituted also by means of the simple spring-mass model. However, in Szolc *et al.* (2010), the circuit model of the asynchronous motor was applied as a torsional excitation source for complex structural models of a heavy working machine drive system.

In the presented paper, the dynamic interaction between mechanical torsional vibrations and electric current vibrations in a precise drive system driven by a stepping motor is modelled. Since in such a case, a possibly exact rotational motion of the mechanism must be assured, the first target of this study is to introduce a sufficiently accurate model of the drive system and of the electric motor, using which the dynamic electromechanical coupling effects are going to be simulated and analysed. The second purpose is to emphasise the importance of the electromechanical coupling on the dynamic interaction between the stepping motor and the drive system, contrary to the traditional approaches mentioned above.

2. Assumptions for the electromechanical model

In the paper, a precise drive system driven by means of a stepping motor, as shown in Fig. 1, is considered. This system consists of the driving motor, direct-current (DC) generator, rotational angle encoder, three elastic couplings of the Oldham-type, inertial ring representing the rotor of the power receiver (impeller), one-stage rubber toothed-belt gear and connecting shaft segments properly supported by roll-bearings. Since the fundamental excitations generated by the driving motor as well as the retarding torques yielded by the power receivers are torsional in character, the torsional vibrations of the drive system are going to be regarded as predominant. Nevertheless, the influence of bending vibrations, which could contribute to the studied dynamic processes, have been also properly examined. In order to investigate the dynamic

coupling effects between the vibrating mechanical drive system and electric vibrations in the motor windings, it is necessary to assume a reasonably realistic and computationally efficient mechanical and electrical model. Thus, in this paper, the structural electromechanical hybrid model of the drive system is going to be applied.

2.1. Hybrid modelling of the mechanical system

In order to perform a theoretical investigation of the electromechanical coupling effects in this system, a reliable and computationally efficient simulation model is required. In this paper, dynamic investigations of the entire drive system are performed by means of the applied, e.g. in Szolc (2000, 2003) and Szolc *et al.* (2010), one-dimensional hybrid (discrete-continuous) model consisting of continuous visco-elastic macro-elements, discrete oscillators and of rigid bodies mutually connected according to the structure of the real object, as shown in Fig. 1. In this model, successive cylindrical segments of the

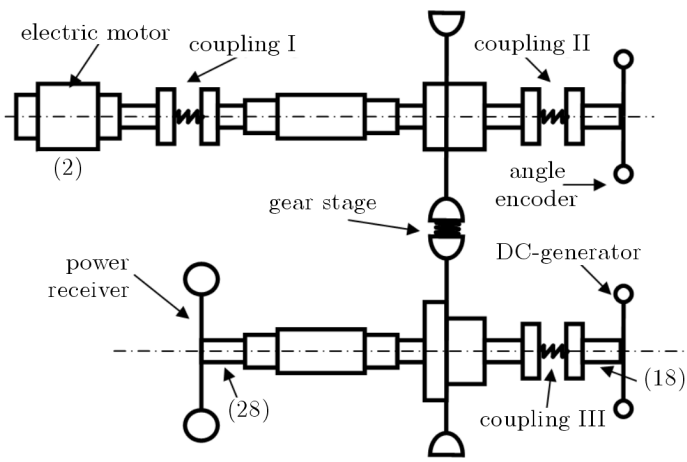

Fig. 1. The hybrid mechanical model of the drive system

stepped shafts are substituted by torsionally deformable cylindrical macro-elements of continuously distributed inertial-visco-elastic properties. Since in the real drive system, the electric motor coils, roll bearing inner rings and gears are attached along some shaft segments by means of the shrink-fit connections, the entire inertia of such components is increased, whereas usually the shaft cross-sections only are affected by elastic deformations due to transmitted loadings. Thus, the corresponding visco-elastic macro-elements in the hybrid model must be characterised by the geometric cross-sectional polar

moments of inertia J_{Ei} responsible for their elastic and inertial properties as well as by the separate layers of the polar moments of inertia J_{Ii} responsible for their inertial properties only, $i = 1, 2, \ldots, n$, where n is the total number of macro-elements in the considered hybrid model, Fig. 1. Moreover, on the actual operation temperature T_i can depend values of Kirchhoff's modulus G_i of the rotor-shaft material of density ρ for each i-th macro-element representing the given shaft segment. In the proposed hybrid model of the drive system, the inertias of the impeller, gears, DC-generator rotor, coupling disks and of the rotational angle encoder rotor are represented by the rigid bodies attached to the appropriate macro-element extreme cross-sections. The macro-elements and rigid bodies can be also connected by means of mass-less torsional springs substituting visco-elastic properties of the gear meshing and of the elastic couplings. Such an approach in the modelling should assure a reasonable accuracy for practical purposes. This hybrid mechanical model is employed here for eigenvalue analyses as well as for numerical simulations of torsional vibrations of the drive train.

Torsional motion of cross-sections of each visco-elastic macro-element is governed by the hyperbolic partial differential equations of the wave type

$$G_i(T_i)J_{Ei}\Big(1+\tau\frac{\partial}{\partial t}\Big)\frac{\partial^2\theta_i(x,t)}{\partial x^2} - c_i\frac{\partial\theta_i(x,t)}{\partial t} - \rho(J_{Ei}+J_{Ii})\frac{\partial^2\theta_i(x,t)}{\partial t^2} = q_i(x,t) \tag{2.1}$$

where $\theta_i(x,t)$ is the angular displacement with respect to the shaft rotation with the average angular velocity Ω, τ denotes the retardation time in the Voigt model of material damping and c_i is the coefficient of external (absolute) damping. The time- and response-dependent external torques can be imposed in the concentrated form on the given shaft cross-sections or continuously distributed along the respective macro-elements of the lengths l_i. These continuously distributed torques are described by the two-argument functions $q_i(x,t)$, where x is the spatial co-ordinate, t denotes time and $i = 1, 2, \ldots, n$.

Mutual connections of the successive macro-elements creating the stepped shaft as well as their interactions with the rigid bodies are described by equations of boundary conditions. These equations contain geometrical conditions of conformity for rotational displacements of the extreme cross sections of the adjacent $(i-1)$-th and the i-th visco-elastic macro-elements. The second group of boundary conditions are dynamic ones, which contain equations of equilibrium for external torques as well as for inertial, elastic and external damping moments. In this hybrid mechanical model, the gear stage and the elastic couplings are also described by the dynamic boundary conditions. Here, the gears and coupling disks are represented by rigid bodies. The connection

of the $(i-1)$-th macro-element with the i-th macro-element is realised by means of the mass-less visco-elastic springs substituting the rubber toothed-belt stiffness of the gear as well as the elastic coupling stiffness.

The proposed hybrid structural model of the drive system is assumed as a linear one, since typically non-linear stiffness characteristics of the elastic couplings or of the rubber belt in the gear stage can be linearised in the expected domains of relatively small dynamic torsional displacements and tangential strains. Moreover, because of commonly applied initial static pre-stress of the rubber toothed-belt in the gear, all backlash effects in the drive system can be assumed as eliminated and neglected in the further dynamic investigations.

In the hybrid model of the considered drive system, the external electromagnetic torque produced by the stepping motor is assumed as continuously and uniformly distributed along macro-element (2) representing its rotor, Fig. 1. The retarding torques generated by the power receiver and the DC-generator are imposed in the concentrated form to rigid bodies (28) and (18) corresponding, respectively, to the rotors of the mentioned drive components.

2.2. Modelling of the electric motor

In the considered drive system, there is applied a quite typical four-cycle, double-phase stepping motor with the fundamental step angle 1.8 deg=0.0314 rad, which means that its rotor is characterised by $Z_r = 50$ poles. According e.g. to Sochocki (1996) and Pochanke and Bodnicki (2002), the mathematical model of such a stepping motor is described by two voltage equations

$$\begin{aligned}
&L_0\frac{di_1(t)}{dt} + Ri_1(t) - K_U\frac{d\Theta(t)}{dt}\sin(\Theta_E(t)) = -U(t)\,\mathrm{sgn}\,\{\sin(\Phi(t))\}\\
&L_0\frac{di_2(t)}{dt} + Ri_2(t) + K_U\frac{d\Theta(t)}{dt}\cos(\Theta_E(t)) = U(t)\,\mathrm{sgn}\,\{\cos(\Phi(t))\}\\
&\Phi(t) = \frac{\pi}{2}\int_0^t f(\tau)\,d\tau
\end{aligned} \tag{2.2}$$

where $i_1(t)$, $i_2(t)$ denote the electric currents in both motor phases, L_0 is the phase inductance, R denotes the resistance of one phase, K_U is the motor voltage constant, $\Theta(t)$ denotes the instantaneous rotation angle of the rotor including the rigid body motion and the vibratory component, $U(t)$ is the slowly varying control voltage, $\Theta_E(t)$ denotes the rotor electric angle, which can be determined as $\Theta_E(t) = Z_r\Theta(t)$ and $f(t)$ is the voltage supply commutation frequency. Here, sufficiently good commutation realised by means of

a proper stepping motor control should result in the control voltage supply phase angle $\Phi(t) \cong \Theta_E(t)$.

The electromagnetic torque generated by the double-phase stepping motor is expressed by the following formula

$$T_E(t) = K_T[-i_1(t)\sin(\Theta_E(t)) + i_2(t)\cos(\Theta_E(t))] \tag{2.3}$$

where K_T denotes the stepping motor torque constant.

3. Mathematical solution of the problem

Torsionally vibrating drive systems are usually characterised by a relatively low level internal and external (absolute) damping. This so commonly observed feature is caused by natural very small material damping in metallic and non-metallic components operating in the range of small tangential strains and torsional displacements. The well lubricated roll-bearings also do not introduce much friction due to shaft rotational motion, and thus the induced external damping can be regarded as negligible. Therefore, torsional natural frequencies and eigenmode functions obtained for the undamped systems are respectively very close to these determined by means of damped eigenvalue problem solution. According to the above, in order to perform an analysis of natural elastic vibrations of the mechanical model, all the forcing and viscous terms in equations of motion (2.1) and in the boundary conditions have been omitted. An application of the solution of variable separation for Eqs. (2.1) leads to the following characteristic equation for the considered eigenvalue problem

$$\mathbf{C}(\omega)\boldsymbol{D} = \mathbf{0} \tag{3.1}$$

where $\mathbf{C}(\omega)$ is the real characteristic matrix and $\boldsymbol{D}$ denotes the vector of unknown constant coefficients in the analytical local eigenfuctions of each i-th macro-element, Szolc (2000, 2003). Thus, the determination of natural frequencies reduces to the search with a required computational accuracy for values of ω, for which the characteristic determinant of matrix $\mathbf{C}$ is equal to zero. Then, the torsional eigenmode functions are obtained by solving equation (3.1). It should be emphasised that for the torsionally vibrating 'free-free' system, apart from the theoretically infinite number of elastic modes, the so called rigid-body mode of zero natural frequency must be taken into consideration.

The solution for forced vibration analysis has been obtained using the analytical-computational approach applied e.g. in Szolc (2000, 2003) and Szolc *et al.* (2010). Solving eigenvalue problem (3.1) and applying the Fourier solution in form of series in the orthogonal eigenfunctions leads to the set of uncoupled modal equations for time coordinates $\xi_m(t)$

$$\ddot{\xi}_m(t) + (\beta + \tau\omega_m^2)\dot{\xi}_m(t) + \omega_m^2\xi_m(t) = \frac{1}{\gamma_m^2}Q_m(t) \qquad m = 0, 1, 2, \ldots \tag{3.2}$$

where ω_m are successive natural frequencies of the drive system, β denotes the coefficient of external damping assumed here as proportional damping to the modal masses γ_m^2 and $Q_m(t)$ are the modal external excitations. By making use of the principle of virtual work, the modal external excitations for the hybrid (discrete-continuous) model of the considered drive system have been determined in the following form $(m = 0, 1, 2, \ldots)$

$$Q_m(t) = \frac{T_E(t)}{l_2}\int_0^{l_2} X_{2m}(x)\,dx - M_{18}(t)X_{18,m}(0) - M_{28}(t)X_{28,m}(l_{28}) \tag{3.3}$$

where $X_{2m}(x)$ denotes the local m-th eigenfunction of macro-element (2) of length l_2 corresponding to the electric motor rotor, $X_{18,m}(0)$, $X_{28,m}(l_{28})$ are the m-th eigenfunction values for the model cross-sections in which there are imposed retarding torques $M_{18}(t)$ and $M_{28}(t)$ generated respectively by the DC-generator and the power receiver. Here, it is assumed that the DC-generator produces a constant or slowly varying with time retarding torque $M_{18}(t) = T_0(t)$ representing dry friction effects in the drive system. The power receiver is assumed to be loaded by aerodynamic forces, and thus the retarding torque imposed on the corresponding inertial disk, see Fig. 1, can be expressed as the square function of the current rotational speed $M_{28}(t) = H\omega^2(t)$, where $\omega(t)$ is the inertial disk instantaneous rotational speed containing the average component together with the fluctuating component due to torsional vibrations of the drive system and H denotes the proper aerodynamic constant coefficient.

By substituting expression (2.3) into (3.3) and (3.2), and upon proper combinations of modal equations (3.2) with voltage equations (2.2), one obtains the coupled set parametric ordinary differential equations

$$\mathbf{M}\ddot{\boldsymbol{r}}(t) + \mathbf{C}(\Theta_E(t))\dot{\boldsymbol{r}}(t) + \mathbf{K}(\Theta_E(t))\boldsymbol{r}(t) = \boldsymbol{F}(t, \dot{\boldsymbol{r}}(t)) \tag{3.4}$$

where

$$\mathbf{C}(\Theta_E(t)) = \mathbf{C}_0 + \mathbf{C}_E(\Theta_E(t)) \qquad \mathbf{K}(\Theta_E(t)) = \mathbf{K}_0 + \mathbf{K}_E(\Theta_E(t))$$

$$\boldsymbol{r}(t) = \operatorname{col}[i_1(t), i_2(t), \xi_0(t), \xi_1(t), \xi_2(t), \ldots]$$

$$\boldsymbol{F}(t, \dot{\boldsymbol{r}}(t)) = \begin{bmatrix} -U(t)\operatorname{sgn}\{\sin(\Phi(t))\} \\ U(t)\operatorname{sgn}\{\cos(\Phi(t))\} \\ -\kappa\,(M_{18}(t) + M_{28}(\dot{\boldsymbol{r}}(t))) \\ -X_{18,1}(0)M_{18}(t) - X_{28,1}(l_{28})M_{28}(\dot{\boldsymbol{r}}(t)) \\ -X_{18,2}(0)M_{18}(t) - X_{28,2}(l_{28})M_{28}(\dot{\boldsymbol{r}}(t)) \\ \ldots \end{bmatrix}$$

The symbols $\mathbf{M}$, $\mathbf{C}_0$ and $\mathbf{K}_0$ denote, respectively, the constant diagonal modal mass, damping and stiffness matrices, $\mathbf{C}_E(\Theta_E(t))$ is the band matrix of the inductive-electro-magnetic effects and $\mathbf{K}_E(\Theta_E(t))$ denotes the band matrix of the resistant-electro-magnetic effects, both of harmonically variable coefficients with the frequency following from the current electric rotation angle. The symbol $\boldsymbol{F}(t, \dot{\boldsymbol{r}}(t))$ denotes the external excitation vector due to the control input voltage and retarding torques. The unknown co-ordinate vector $\boldsymbol{r}(t)$ consists of electric currents in both motor phases and of the unknown time functions $\xi_m(t)$ in the Fourier solutions, $m = 0, 1, 2, \ldots$. In order to obtain the system dynamic response, equations (3.4) are solved by means of direct integration using Newmark's method. The number of equations (3.4) corresponds to the number of eigenmodes taken into consideration in the range of frequency of interest. These equations are mutually coupled by the parametric terms expressing to the electromagnetic interaction with the stepping motor. A fast convergence of the applied Fourier solutions enables us to reduce the appropriate number of the modal equations to solve, in order to obtain a sufficient accuracy of results in the given range of frequency. In such a frequency range, mutual overlying of the frequency response functions determined for the given, gradually increased number of considered eigenmodes can be used as an additional accuracy test for the proper mode truncation.

In this way, the electro-mechanical hybrid model of the drive system has been obtained. It is to remark that a natural alternative for dynamic modelling of the considered drive system is application of the classical finite element method. Then, in a comparison with the proposed here hybrid (discrete-continuous) model, in such a case the general structure of the finite element mechanical model would be exactly the same, where only the visco-elastic macro-elements used in the hybrid model must have been discretized by means of one-dimensional torsionally deformable two-node finite elements of the rod-type, but all rigid bodies and discrete-oscillators would remain unchanged. Such an analogous finite element and hybrid models of the drive system were

developed in Szolc *et al.* (2010). From comparison of results of eigenproblem analyses performed by means of both models, it follows that using the finite element method it is possible to obtain very close natural frequency values and almost identical eigenforms as in the case of the hybrid model upon thorough selection of proper discretization mesh densities resulting usually in relatively large numbers of degrees of freedom of the entire finite element model, Szolc *et al.* (2010). Then, simulations of forced vibrations carried out by the use of these models can yield very similar results. But in the case of the hybrid model, it is necessary to solve only few coupled modal equations (3.4), even in cases of great and complex mechanical systems, contrary to the classical one-dimensional finite element formulation leading usually to large numbers of equations of motion corresponding each to more than one hundred or many hundreds degrees of freedom, (if artificial and often error prone model reduction algorithms are not applied). However, the proposed here hybrid modelling assures at least the same or even better representation of the real object as well as its mathematical description is formally strict, demonstrates clearly qualitative system properties and is much more convenient for a stable and efficient numerical simulation.

4. Computational examples

In the computational examples, simulations of the run-up, steady state operation and run-down of the existing in practice laboratory precise geared drive system are performed. The mechanical model is shown in Fig. 1 and its detailed parameters are taken form technical documentation. It is to emphasise that the proposed hybrid model is characterised by respectively identical geometrical and physical parameters as the mentioned in Section 3 analogous finite element model of the same structure. In this way, both models yield the same level of parameter identification errors. The considered drive system is driven by means of the stepping motor of the nominal voltage 4.8 V, current 1.5 A and the maximal braking torque 0.8 Nm, where the reduction gear ratio is equal to 1:3. In each case of the assumed operation parameters this mechanical system of the entire mass moment of inertia reduced to the motor axis $9.34 \cdot 10^{-5}\,\mathrm{kgm}^2$ was uniformly accelerated from its standstill to the constant average rotational speed within $t_1 = 3\,\mathrm{s}$ in order to operate for next $t_2 - t_1 = 1\,\mathrm{s}$ under the constant retarding torque generated by the generator. Then, within successive $t_3 - t_2 = 3\,\mathrm{s}$, the drive system was uniformly stopped back to the standstill.

The four following cases of the drive system operation parameters are going to be investigated:

1. The nominal rotational speed $n = 1500\,\text{rpm}$ $(25\,\text{s}^{-1})$ and the suddenly applied nominal retarding torque $T_0 = 0.03\,\text{Nm}$;
2. The nominal rotational speed $n = 600\,\text{rpm}$ $(10\,\text{s}^{-1})$ and the suddenly applied nominal retarding torque $T_0 = 0.10\,\text{Nm}$;
3. The nominal rotational speed $n = 300\,\text{rpm}$ $(5\,\text{s}^{-1})$ and the gradually applied during start-up and run-down nominal retarding torque $T_0 = 0.35\,\text{Nm}$;
4. The nominal rotational speed $n = 210\,\text{rpm}$ $(3.5\,\text{s}^{-1})$ and the gradually applied during start-up and run-down nominal retarding torque $T_0 = 0.35\,\text{Nm}$.

In all four cases, the identical absolute damping coefficient $\beta = 6 \cdot 10^{-5}\,\text{Nms}$, the aerodynamic constant coefficient $H = 4 \cdot 10^{-7}\,\text{Nms}^2$ and the retardation time for steel in the Voigt model of material damping $\tau = 2.34 \cdot 10^{-5}\,\text{s}$ have been assumed.

In order to study the influence of electro-mechanical coupling effects on dynamic responses of the considered system, numerical simulations of the assumed above motions have been carried out for two modes: (a) – for the "coupled simulation mode", where the full electro-mechanical system described by equations (3.4) was used, and (b) – for the so called "uncoupled simulation mode", where according to the commonly applied approach in the literature, e.g. in Sochocki (1996), only two following electrical equations coupled with the equation describing the rigid body motion of the drive train were used

$$\begin{aligned}
&L_0\frac{di_1^*(t)}{dt} + Ri_1^*(t) - K_U\frac{d\xi_0^*(t)}{dt}\sin(Z_r\xi_0^*(t)) = -U(t)\,\text{sgn}\{\sin(\Phi(t))\}\\
&L_0\frac{di_2^*(t)}{dt} + Ri_2^*(t) + K_U\frac{d\xi_0^*(t)}{dt}\cos(Z_r\xi_0^*(t)) = U(t)\,\text{sgn}\{\cos(\Phi(t))\}\\
&\gamma_0^2\frac{d^2\xi_0^*(t)}{dt^2} + \beta\frac{d\xi_0^*(t)}{dt}\\
&\quad = K_T[i_2^*(t)\cos(Z_r\xi_0^*(t)) - i_1^*(t)\sin(Z_r\xi_0^*(t))] - T_0(t) - F\Omega^2(t)
\end{aligned} \tag{4.1}$$

where $i_1^*(t)$, $i_2^*(t)$ denote the electric currents in both motor phases and $\xi_0^*(t)$ is the rotational coordinate corresponding to the system rigid body motion. Then, in the case of uncoupled mode, electromagnetic torque (2.3) is *a priori* determined for $i_1^*(t)$, $i_2^*(t)$ and $\xi_0^*(t)$ and substituted into separate modal motion equations (3.2) as a response-independent external excitation of the mechanical system under torsional vibrations.

Example I: The nominal rotational speed $n = 1500\,\mathrm{rpm}$ $(25\,\mathrm{s}^{-1})$ and the suddenly applied nominal retarding torque $T_0 = 0.03\,\mathrm{Nm}$

In the first computational example, the drive system was quickly accelerated to a relatively high average rotational speed under suddenly applied constant loading determined by the maximal motor power limit. In Figs. 2, 3 and 4, plots of the computational results obtained for this case of operation are demonstrated. In Figs. 2, 3 and 4, by black and grey lines, the responses

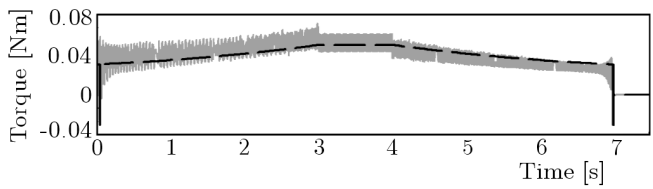

Fig. 2. The retarding (dashed line) and electro-magnetic torque for the coupled (black line) and uncoupled (grey line) simulation mode

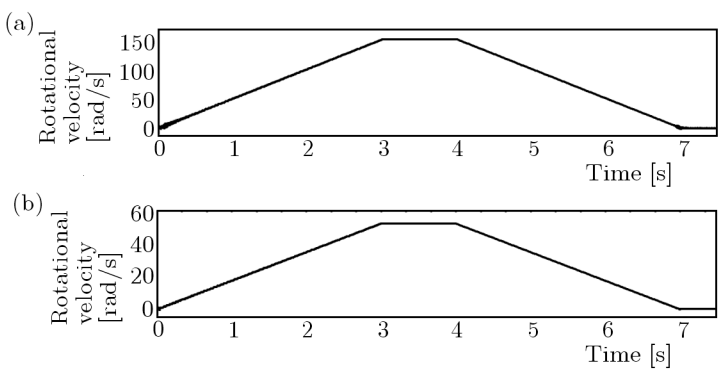

Fig. 3. The rotational velocity of the input (a) and the output (b) shaft for the coupled (black line) and uncoupled (grey line) simulation mode

corresponding respectively to the coupled and uncoupled mode are depicted. In Fig. 2, time-history plots of the electro-magnetic torque generated by the stepping motor as well as of the resultant retarding torque reduced on the motor shaft (denoted by the dashed line) are presented. From this figure it follows that the motor torque time-histories obtained for the coupled and uncoupled mode almost overlay each other. Moreover, for the assumed relatively high average nominal rotational speed, the influence of the retarding aerodynamic torque imposed on the inertial disk of the power receiver as well as the viscous resistance in the system are quite significant. It is to remark that also almost

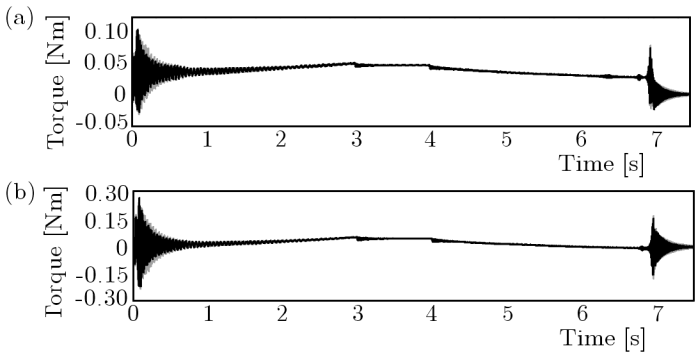

Fig. 4. The dynamic torque transmitted by the input (a) and by the output (b) shaft for the coupled (black line) and uncoupled (grey line) simulation mode

identical responses for the coupled and uncoupled mode have been obtained for rotational speeds of the system input and output shaft segments, where the vibratory components of the angular velocity are negligible, Fig. 3. However, some slight differences are observed in Figs. 4a and 4b demonstrating time-history plots of the dynamic torques transmitted by the system input and output shafts in resonance zones of the first system natural frequency equal 103.4 Hz passed during the start-up and run-down. These differences are characterised only by a little bit slower decaying intensity of transient resonance amplitudes in the case of uncoupled mode.

Example II: The nominal rotational speed $n = 600\,\text{rpm}$ $(10\,\text{s}^{-1})$ and the suddenly applied nominal retarding torque $T_0 = 0.10\,\text{Nm}$

In the second computational example, the drive system was accelerated to a smaller average rotational speed under suddenly applied constant loading, which – from the viewpoint of the abovementioned power limit – could be assumed greater than in the previous case. From the computational results obtained in this case, but not presented in the graphical form, it follows that the motor torque time-histories obtained for the coupled and uncoupled mode begin to not overlay each other during start-up and run-down. Analogous differences are observed for rotational speeds and dynamic torques registered for the considered input and output shaft segments. However, during steady-state operation, the electromagnetic motor torque as well as the system dynamic response in the form of investigated rotational speeds and dynamic torques mutually almost overlay respectively for the coupled and uncoupled mode. This fact can be preliminarily explained by a more vibratory character of system

operation in the considered example because of a smaller gradient of excitation frequency caused by passages through the resonance zone to a much smaller nominal rotational speed during start-up and back to the standstill during run-down as well as due to rapid loading and release by the constant retarding torque T_0 of more than three times greater value than in the previous case. The observed differences between the excitation torques and the system dynamic responses registered for the coupled and uncoupled mode will become much more severe in the next studied cases of the drive system operation described in the two next points.

Example III: The nominal rotational speed $n = 300\,\mathrm{rpm}$ $(5\,\mathrm{s}^{-1})$ and the gradually applied and released nominal retarding torque $T_0 = 0.35\,\mathrm{Nm}$

In this case, the drive system was accelerated to a relatively small nominal rotational speed $n = 300\,\mathrm{rpm}$ $(5\,\mathrm{s}^{-1})$ within 3 s, which resulted in an appropriately lower than before average acceleration and deceleration and in associated with it smaller inertial resistances. Also the applied aerodynamic and viscous retarding torques became almost negligible. However, in comparison with the maximal starting moment of the considered stepping motor equal to 0.5 Nm, the relatively high nominal retarding torque $T_0 = 0.35\,\mathrm{Nm}$ must have been gradually imposed and released in order to assure fluent operation of the drive system.

The corresponding time-history plots of the electromagnetic torque generated by the stepping motor as well as of the resultant retarding torque reduced on the motor shaft (denoted by the dashed line) are presented in Fig. 5. Similarly as in the previous computational example described in Example II, it follows from this figure that the motor torque time-histories obtained for the coupled and uncoupled modes do not overlay each other during start-up and run-down. Moreover, they are also characterised by the remarkable differences in the nominal operation conditions. Significantly greater amplitudes of the excitation electromagnetic torque occur for the coupled mode during the start-up and run-down, however within the steady-state operation, a more regular time-history with slightly greater amplitudes is observed for the motor torque generated in the case of the uncoupled mode.

In Figs. 6 and 7, in exactly the same way as in Example I, time-history plots of the registered system dynamic response are shown. During the start-up and run-down, the rotational velocities as well as the dynamic torques observed in the system input and output shaft are characterised by severe transient resonances with the fundamental eigenmode of the first natural frequency equal 103.4 Hz, as shown in Figs. 6 and 7. The amplitudes of this resonances are

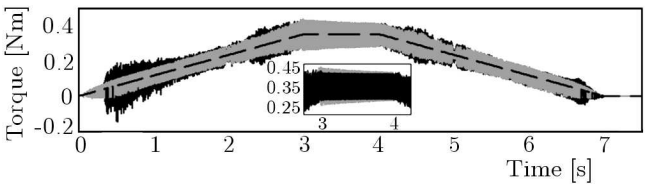

Fig. 5. The retarding (dashed line) and electro-magnetic torque for the coupled (black line) and uncoupled (grey line) simulation mode

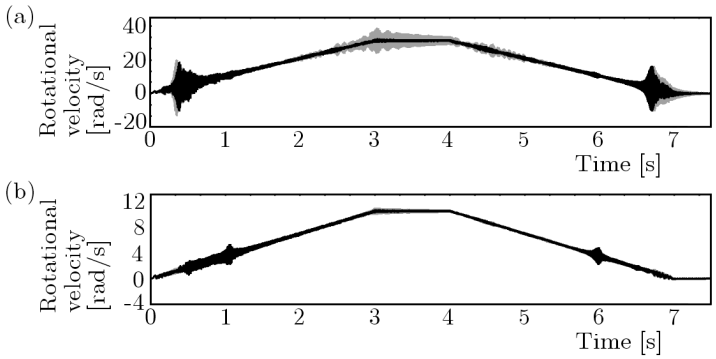

Fig. 6. The rotational velocity of the input (a) and the output (b) shaft for the coupled (black line) and uncoupled (grey line) simulation mode

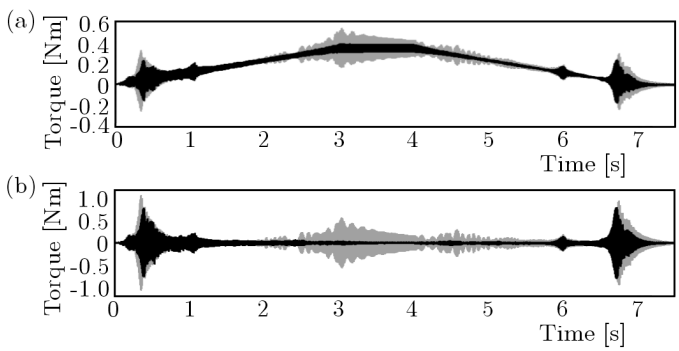

Fig. 7. The dynamic torque transmitted by the input (a) and the output (b) shaft for the coupled (black line) and uncoupled (grey line) simulation mode

respectively similar to each other in the case of the coupled and uncoupled mode, although in these operation conditions, the coupled mode yield much more severe external excitation produced by the driving motor, which follows from Fig. 5. However, during the steady-state operation in the case of the uncoupled mode, the abovementioned regular and slightly stronger electromagnetic excitation results in resonant responses both for the rotational speeds and the

dynamic torques, which have been illustrated in Figs. 6a and 7a,b. In order to explain this fact the FFT analysis of the time-histories of the excitation torque generated by the stepping motor has been performed for the coupled and uncoupled mode.

The obtained in this way amplitude spectra are presented in Fig. 8. From this figure it follows that both amplitude spectra, i.e. the obtained for the coupled mode and depicted by the black line and for the uncoupled mode depicted by the grey line, are characterised by almost identical greatest peaks of frequency 1000 Hz corresponding to the fundamental excitation component produced by the driving motor in steady-state operation conditions. This value results from the assumed nominal rotational speed $n = 300\,\text{rpm}$ $(5\,\text{s}^{-1})$ and the fundamental step angle 0.0314 rad of the considered motor.

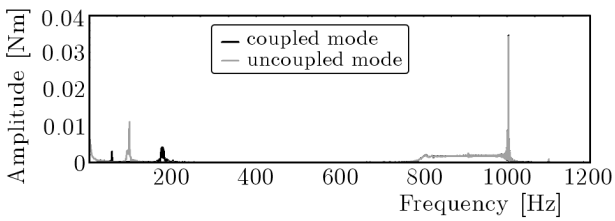

Fig. 8. Amplitude spectra of the excitation torque generated by the stepping motor

Here, for the coupled and uncoupled mode, the excitation motor torque has been determined using two different systems of parametric ordinary differential equations. In the case of the coupled mode, electromagnetic torque (2.3) follows from the system of parametric equations (3.4) taking into consideration the rigid body motion together with the inertial-visco-elastic behaviour of the drive system. However, in the case of the uncoupled mode, electromagnetic torque (2.3) has been determined using the system of parametric equations (4.1) taking into consideration the system rigid body motion only. Thus, by means of these two different parametric systems of equations, apart from the mentioned above identical fundamental components of frequency 1000 Hz, different sub-harmonic components of the excitation torque are generated. In the case of the uncoupled mode, in Fig. 8 the significant excitation component of frequency ca. 100 Hz is observed, which is very close to the first drive system natural frequency equal to 103.4 Hz. This component is responsible for the observed resonance effects depicted in Figs. 6 and 7 for the uncoupled mode, in contradistinction to the coupled mode, where the analogous sub-harmonic excitation component is characterised by frequency ~ 200 Hz, which is far away from the first and the second system natural frequency equal to 344.4 Hz. According to the above, one can conclude that the taken into consideration vibratory,

inertial-visco-elastic properties of the mechanical system essentially influence, both qualitatively and quantitatively, the electromechanical coupling effects resulting respectively in different dynamic responses. This remark will be confirmed in the next computational example in a more profound way.

Example IV: The nominal rotational speed $n = 210\,\mathrm{rpm}$ $(3.5\,\mathrm{s}^{-1})$ and the gradually applied and released nominal retarding torque $T_0 = 0.35\,\mathrm{Nm}$

This example differs from the previous one by the value of the nominal rotational speed equal to $n = 210\,\mathrm{rpm}$ $(3.5\,\mathrm{s}^{-1})$ with all the remaining drive system operation parameters unchanged. It results in a lower average acceleration during start-up and in a lower average deceleration during run-down, and in this way, in smaller gradients of the excitation frequency during passages through the zone of resonance with the first eigenvibration mode. From the computational results obtained in this case, but also not presented in a graphical form, it follows that the transient resonance amplitudes are greater than in the previous example because of the mentioned above smaller gradients of the excitation frequency during passages through the resonance zone within the start-up and run-down time, both for the coupled and uncoupled simulation mode. However, in this example, in the case of the uncoupled mode at the end of the nominal steady-state operation and at the beginning of the system run-down, a very severe resonance is observed for responses investigated in the system input and output shafts. The reason of such behaviour is the same as that described in Ezample III since the amplitude spectra of the driving motor torques obtained in this case and presented in Fig. 9 are analogous to these presented in Fig. 8. In the considered example, in the case of the uncoupled mode by means of parametric system of equations (4.1), there is still generated the sub-harmonic external excitation component of frequency ca. 100 Hz, which induces this extremely severe resonance with the drive system fundamental eigenmode of the first natural frequency 103.4 Hz. In the case of the coupled mode, the analogous sub-harmonic excitation component is also characterised by frequency close to $\sim 200\,\mathrm{Hz}$, which as above mentioned is far away from the first and second system natural frequency equal to 344.4 Hz, see Fig. 9. Thus, in the case of the coupled simulation mode, such a resonance effect at the end of the nominal steady-state operation and at the beginning of the system run-down did not occur.

In order to make knowledge about the reasons of such dynamic behaviour of the considered drive system deeper, several numerical simulations have been performed for other various retarding torques T_0 and for other nominal rotational speeds within the range 100-1500 rpm $(1.67\text{-}25\,\mathrm{s}^{-1})$. From the

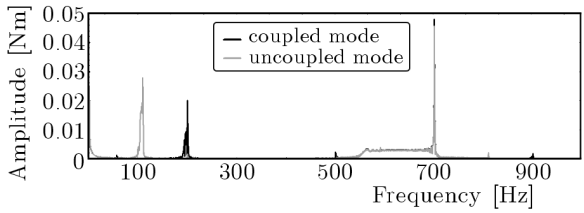

Fig. 9. Amplitude spectra of the excitation torque generated by the stepping motor

FFT analyses of time-histories of the electro-magnetic stepping motor torques obtained in all these simulation cases it follows that this excitation is characterised by "rich" amplitude spectra of frequency components, both in the case of coupled and uncoupled simulation modes. The excitation motor torque component of frequency $\sim 100\,\mathrm{Hz}$, which induced resonances in the case of the uncoupled mode in Examples III and IV, always occurred in the range of nominal rotational speeds between 100-400 rpm (1.67-6.67 s^{-1}). It was not observed for greater nominal rotational speeds, neither in the case of the uncoupled mode nor for the coupled simulation mode. In the case of the coupled mode, this excitation component did not appear also in the nominal rotational speed range 100-400 rpm, similarly as for 300 and 210 rpm (5 and 3.5 s^{-1}) assumed respectively in Examples III and IV. This fact can be explained by natural self-detuning of the coupled electro-mechanical system from the resonance, where a relatively severe rotational speed fluctuation of the stepping motor rotor mistunes "rhythmic" energy supply from the electric motor to the mechanical system, which results in "escaping" of the mechanical system from the parametric resonance. However, in the case of the uncoupled simulation mode, the frequencies of the electro-magnetic excitation torque fluctuation are independent of mechanical visco-elastic vibrations of the drive system and, in this way, also independent of vibratory rotational speed oscillations of the motor rotor. Thus, the given excitation frequency is able to correspond permanently to the given natural frequency of the mechanical system, e.g. to the first one as in the considered here object, and then some artificial resonance effects can be induced.

5. Conclusions

In the paper, electro-mechanical vibrations of the drive system driven by the stepping motor have been investigated. These investigations have been performed by means of the entirely coupled electro-mechanical model of the considered object as well as using the traditional approach based on the mutually

uncoupled mechanical and electrical system. In the coupled model, torsional vibrations of the drive system and electric current oscillations in the motor windings have been taken into consideration in form of a common set of parametric ordinary differential equations containing the modal equations of motion for the mechanical part and the circuit equations describing operation of the electric motor. In contradistinction to the approaches usually applied till present, where the electric and mechanical parts of the drive systems cooperating with the electric machines are studied separately from each other or one of them, e.g. the mechanical one, is drastically simplified, the proposed electro-mechanical model enables us to consider all required mechanical and electrical properties of the investigated object in order to obtain an expected level of accuracy.

In the case of the coupled simulation mode, the rigid body motion together with the vibratory behaviour of the mechanical system influence the electric currents in the motor windings, which are responsible for generation of the electromagnetic excitation torque. However, in the case of the uncoupled mode, the electromagnetic excitation torque is generated by solving the motor voltage equations coupled only with the equation describing the rigid body motion of the mechanical system. Then, the electromagnetic motor torque has been a priori' substituted into the modal equations of vibratory motion. According to the above, the electromagnetic torques generated by the stepping motor were characterised by different frequency components in the case of coupled and uncoupled modes.

The performed investigations enabled us to indicate essential qualitative and quantitative differences between the computational results obtained using the coupled and uncoupled mode of the vibrating electro-mechanical drive system. In the case of the traditional uncoupled mode, the electromagnetic torque generated by the considered stepping motor contained an excitation component of a frequency very close to the first natural frequency of the drive system, which was not observed using the coupled mode. Thus, in the dynamic responses obtained by means of the uncoupled mode, severe "artificial" resonance effects have been induced.

From the comparison of the computational results obtained for the four considered cases of operational parameters, it follows that the most severe coupled electro-mechanical dynamic responses were observed in Example II, III and IV, in which the drive system was accelerated to relatively smaller nominal rotational speeds and loaded by appropriately much greater retarding torques produced by the DC-generator. Then, due to larger transmitted loadings and smaller gradients of instantaneous excitation frequency caused by passa-

ges through the system resonance zone during start-ups and run-downs, when much stronger transient resonance effects were induced, the responses were characterised by much more severe torsional and electrical vibrations. However in Example I, in which the obtained dynamic response was almost free of vibratory effects, the traditional approach based on the mutually uncoupled mechanical and electrical system yielded similar results to these obtained using the coupled mode. Thus, such results can be regarded as satisfactorily exact. According to the above, for simulations of drive system operations under severe vibrations, the entirely coupled electro-mechanical model is necessary, in particular when sufficiently accurate simulation results are required.

Acknowledgement

These investigations are supported by the Polish National Centre of Research and Development of the Ministry of Science and Higher Education: Research Project PBR-N R03 0012 04.

References

1. Berger H., Kulig T. S., 1981, Simulation models for calculating the torsional vibrations of large turbine-generator units after electrical system faults, *Siemens Forsch. - u. Entwickl. Ber.*, **10**, 4, 237-245
2. Evans B.F., Smalley A.J., Simmons H.R., 1985, Startup of synchronous motor drive trains: the application of transient torsional analysis of cumulative fatigue assessment, *ASME Paper*, 85-DET-122
3. Holopainen, T.P., Repo, A.-K., Järvinen, J., 2010, Electromechanical interaction in torsional vibrations of drive train systems including an electrical machine, *Proc. of the 8th IFToMM Int. Conference on Rotordynamics*, KIST, Seoul, Korea, 986-993
4. Iwatsubo T., Yamamoto Y., Kawai R., 1986, Start-up torsional vibration of rotating machine driven by synchronous motor, *Proc. of the International Conference on Rotordynamics*, IFToMM, Tokyo, Japan, 319-324
5. Laschet A., 1988, *Simulation von Antriebssystemen*, Springer-Verlag, Berlin, Heidelberg, London, New-York, Paris, Tokyo
6. Pochanke A., Bodnicki M., 2002, Modelling of torque meters and measuring system for testing of stepping motors, *Electromotion*, **9**, 4, 210-216
7. Repo, A.-K., Rasilo, P., Arkkio, A., 2008, Dynamic electromagnetic torque model and parameter estimation for a deep-bar induction machine, *Electric Power Applications, IET*, **2**, 3, 183-192

8. Schwibinger P., Nordmann R., 1989, Improvement of a reduced torsional model by means of parameter identification, *Transactions of the ASME, J. of Vibration, Acoustics, Stress and Reliability in Design*, **111**, 17-26

9. Sochocki R., 1996, *Electrical Micro-machines*, 1996, Eds. of the Warsaw University of Technology, Warsaw, ISBN 83-86569-84-0 [in Polish]

10. Szolc T., 2000, On the discrete-continuous modeling of rotor systems for the analysis of coupled lateral-torsional vibrations, *Int. Journal of Rotating Machinery*, **6**, 2, 135-149

11. Szolc T., 2003, Dynamic analysis of complex, discrete-continuous mechanical systems, Polish Academy of Sciences – IFTR Reports, 2/2003, Habilitational dissertation [in Polish]

12. Szolc, T., Jankowski, Ł., Pochanke, A., Magdziak, A., 2010, An application of the magneto-rheological actuators to torsional vibration control of the rotating electro-mechanical systems, *Proc. of the 8th IFToMM Int. Conference on Rotordynamics*, KIST, Seoul, Korea, 488-495

Badanie efektów dynamicznych sprzężeń elektromechanicznych w mechaniźmie napędzanym silnikiem skokowym

Streszczenie

W pracy przeprowadzono analizę przejściowych i ustalonych drgań elektromechanicznych precyzyjnego układu mechanicznego napędzanego silnikiem skokowym. Badania teoretyczne wykonano za pomocą hybrydowego modelu strukturalnego układu napędowego oraz klasycznego obwodowego modelu silnika skokowego. Głównym celem dokonanego studium było wykazanie istotnych różnic pomiędzy odpowiedziami dynamicznymi drgającego skrętnie obiektu traktowanymi jako elektromechanicznie sprzężone i rozprzężone. Na podstawie uzyskanych wyników można stwierdzić, że te różnice są jakościowo i ilościowo znaczące z punktu widzenia precyzyjnego i niezawodnego działania układu napędowego. Wykazano, iż drgania skrętne układu napędowego istotnie wpływają na efekt sprzężenia elektromechanicznego, co uzasadnia ważność jego uwzględniania przy przeprowadzaniu tego typu analiz.

Manuscript received August 13, 2011; accepted for print November 17, 2011